Journal of Sound and Vibration 325 (2009) 907–922

Contents lists available at ScienceDirect

Journal of Sound and Vibration

journal homepage: www.elsevier.com/locate/jsvi

Dynamic response analysis of suspended beams subjected to moving vehicles and multiple support excitations

J.D. Yau

Department of Architecture, Tamkang University, Taipei 10620, Taiwan

ARTICLE INFO

Article history:
Received 2 September 2007
Received in revised form
24 December 2007
Accepted 4 April 2009
Handling Editor: L.G. Tham
Available online 17 May 2009

ABSTRACT

For dynamic analysis of a suspended beam subject to the simultaneous action of moving oscillators and multiple support motions, we need to deal with nonlinear interaction problems in conjunction with *time-dependent* boundary conditions. In this study, the total response of the suspended beam is decomposed into two parts: the *pseudo-static* response and the *inertia-dynamic* component. Then, the *pseudo-static* displacement is analytically obtained by exerting the support movements on the suspended beam statically and the governing equations in terms of the *inertia-dynamic* component as well as moving oscillators are transformed into a set of coupled generalized equations by Galerkin's method. Instead of solving the coupled equations containing *pseudo-static* support excitations and moving oscillators, this study treats all the nonlinear coupled terms as pseudo forces and solves the decoupled equations using the Newmark method with an incremental-iterative approach. Numerical investigations demonstrate that the present solution technique is available in dealing with the vehicle/bridge interaction problem involving multiple support motions, and that appropriate adjustments of cable sag ratios subject to the condition of identical bridge frequencies are beneficial for mitigating the earthquake-induced vibration of suspended bridge/vehicle coupling system.

1. Introduction

Concerning seismic wave propagation effect in subsoil, the dynamic response analysis of long-span structures like suspension bridges needs to deal with the time-dependent boundary problem involving multiple support seismic inputs. For earthquake-induced response analysis of suspension bridges [1–5], an analytical model based on *linearized* deflection theory [6,7] was usually adopted to formulate the governing equations of vertical vibration of suspended bridges. One of concrete indications in these studies is that the multiple support seismic excitations, especially for the longitudinal ground motions along bridge span, have to be taken into account for the earthquake-induced vertical vibration of suspension bridges. On the other hand, many researchers have studied the vehicle-induced vibration of suspension bridges in recent years [8–12]. A key finding in these researches revealed that the cable tensions of *short or medium span* suspension bridges caused by moving loads would be amplified significantly.

For train-induced vibration of rail bridges, Yang et al. [13,14] presented a useful resonant condition to predict or keep away from the resonant speeds for high-speed trains passing over bridges. Concerning the stability problem of a train moving over a bridge shaken by earthquakes, Yang et al.'s book [13] pointed out that the presence of vertical ground excitations would affect drastically the stability of the train, especially for near resonant excitations. Xia et al. [15] revealed

E-mail address: jdyau@mail.tku.edu.tw

0022-460X/$ - see front matter © 2009 Elsevier Ltd. All rights reserved.
doi:10.1016/j.jsv.2009.04.013

that for a train traveling over a continuous seven-span viaduct shaken by earthquakes, lack of considering seismic traveling wave effect might reduce the running safety of the train.

Of the large amount of literatures devoted to vibrations of long-span bridges, relatively little research attention so far seems to conduct the dynamic interaction response of suspension bridges to moving vehicles during earthquakes. Generally speaking, the dynamic interaction behavior of vehicle–bridge system shaken by earthquakes is of a complicated structure problem since it involves a time-dependent boundary vibration problem due to multiple support motions [13,15] and the interaction dynamics of vehicle–bridge coupling system. Considering the non-uniform characteristics of seismic wave propagation, this study intends to investigate the dynamic interaction response of a suspension bridge subject to train loadings during earthquakes. The coupled equations of motion for vehicle–bridge system are formulated using a dynamic interaction model of a single-span suspended beam carrying multiple moving oscillators. To conduct this time-dependent boundary and coupling vibration problem, the total response of the suspended beam is decomposed into two parts: the *pseudo-static* and *inertia-dynamic* components [16–18]. Then, a closed form solution for the *pseudo-static* displacement is presented, while the *inertia-dynamic* deflection is expressed as a set of generalized coordinates in conjunction with admissible shape functions and solved using Galerkin's method. Instead of solving the coupled equations for the generalized system containing *pseudo-static* support excitations and moving oscillators, this study treats all the nonlinear coupled terms as pseudo forces and solves the decoupled equations using the Newmark method with an incremental-iterative procedure involving three phases: *predictor*, *corrector*, and *equilibrium-checking*.

According to the present studies, the inclusion of seismic ground motions will totally amplify both the acceleration responses of suspended beams and moving oscillators, especially for the non-uniform characteristics of seismic wave included. Despite of this fact, a parametric investigation indicates that appropriate adjustments of suspended cables by increasing cable sag but reducing cable stiffness are available in mitigating the acceleration response of the vehicle–bridge system during earthquakes.

2. Formulation

The dynamic behavior of suspension bridges investigated herein is limited to the vertical vibration of a single-span suspended beam with hinged supports. Based on the deflection theory [6,7,19], which can take into account the additional cable tension of a suspended beam due to live loads, appreciable simplifications for the suspended beam and moving trains over it are outlined as follows:

(1) The stiffening girder is modeled as a linear elastic Bernoulli-Euler beam with uniform cross section.
(2) As shown in Fig. 1, the bridge towers supporting the stiffening girder and suspension cable are assumed so rigid that their deformations during vibrations are negligible.
(3) The cable sag is adjustable between the suspension cable and bridge deck.
(4) The suspension cable is assumed to be capable of carrying all the dead loads of the stiffening girder with the aid of inextensible vertical hangers so that the suspended beam is in an un-stressed state before the action of live loads.
(5) The train loadings running over the suspended beam are modeled as a sequence of equidistant moving oscillators with identical properties.

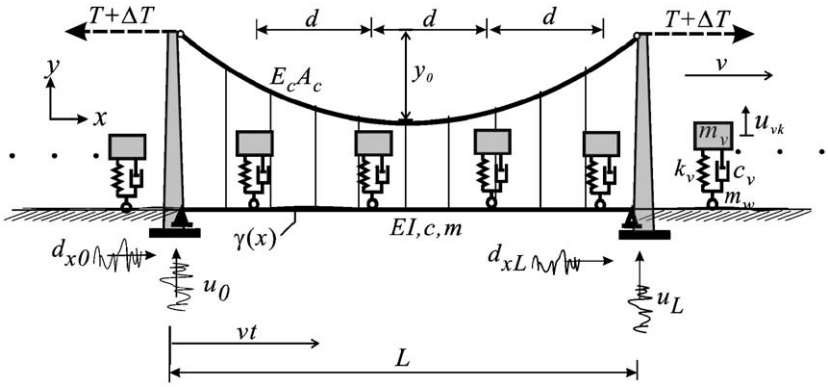

Fig. 1. A suspended beam subject to train loadings and multiple support motions.

2.1. Governing equations of motion

Consider a parabolic cable under a uniform dead load w alone, the cable sag function $y(x)$ and the horizontal component T in the tensile cable can be expressed as [20]

$$y(x) = 4y_0[x/L - (x/L)^2], \tag{1}$$

$$T = \frac{-w}{y''} = \frac{wL^2}{8y_0}, \tag{2}$$

where y_0 is the cable sag at mid-span and L the span length. Based on the *deflection theory* of small deformations for suspension bridges [6,7,19], the equation of vertical vibration is

$$m\ddot{u} + c\dot{u} + EIu'''' - (T + \Delta T)(y'' + u'') = w + p(x,t), \tag{3}$$

where $(\cdot)' = \partial(\cdot)/\partial x$, $(\dot{\cdot}) = \partial(\cdot)/\partial t$, m is the mass of the beam and cable per unit length along x-axis, c the damping coefficient, $u(x,t)$ the vertical deflection of the beam, EI the flexural rigidity of the beam, T the horizontal component in the initial cable tension (due to dead loads), ΔT the additional horizontal component in cable force due to external loads, $u(x,t)$ the beam deflection, and $p(x,t)$ the loading function of moving oscillators. Consider the multiple seismic support movements depicted in Fig. 1, the time-dependent boundary conditions for the suspended beam with hinged ends are given as follows:

$$u(0,t) = u_0(t), \quad u(L,t) = u_L(t),$$

$$EIu''(0,t) = EIu''(L,t) = 0,$$

$$u_x(0,t) = d_{x0}(t), \quad u_x(L,t) = d_{xL}(t), \tag{4}$$

where (u_0, u_L) and (d_{x0}, d_{xL}) represent the vertical and horizontal support movements at the left and right bridge towers, respectively. By considering the support movements, the additional horizontal component ΔT for cable force can be described as [20]

$$\Delta T = \frac{E_cA_c}{L_c}\left[u_x|_0^L + \int_0^L y'u'\,dx\right] = \frac{E_cA_c}{L_c}\left[(d_{xL} - d_{x0}) - \frac{4y_0}{L}(u_0 + u_L) + \frac{8y_0}{L^2}\int_0^L u\,dx\right], \tag{5}$$

$$L_c = \int_0^L \left(\frac{ds}{dx}\right)^3 dx = \int_0^L \left(\sqrt{1+y'^2}\right)^3 dx, \tag{6}$$

in which E_c is the elastic modulus of the cable, A_c the area of the cable, and L_c the effective length of the cable. Substituting Eqs. (1), (2) and (5) into Eq. (3) yields the following equation of motion for a suspended beam subject to the simultaneous action of moving oscillators and seismic support inputs

$$m\ddot{u} + c\dot{u} + EIu'''' - (T + \Delta T_s)u'' + (\alpha + \kappa u'')\int_0^L u\,dx = p(x,t) + \frac{\alpha L}{2}[u_0 + u_L] - \kappa(d_{xL} - d_{x0}), \tag{7}$$

where

$$\Delta T_s = \frac{E_cA_c}{L_c}\left[(d_{xL} - d_{x0}) - \frac{4y_0}{L}(u_0 + u_L)\right], \tag{8a}$$

$$\alpha = \left(\frac{8y_0}{L^2}\right)^2 \frac{E_cA_c}{L_c}, \quad \kappa = \left(\frac{8y_0}{L^2}\right)\frac{E_cA_c}{L_c}. \tag{8b,c}$$

Since the increment of horizontal component of cable force in Eq. (5) is dependent on both the beam deflection $u(x,t)$ and support movements $(u_0, u_L, d_{xL}, d_{x0})$, the governing equation of motion in Eq. (7) is nonlinear in nature. As can be seen from Eq. (7), the coefficient $\alpha + \kappa u''$ in Eq. (7), generally, can be approximated as $\alpha + \kappa u'' = \kappa(8y_0/L^2 + u'') \simeq \alpha$ based on the deflection theory of small amplitudes, i.e., $|u''| \ll |y''| = 8y_0/L^2$. As a result, this approximation will be adopted in the following formulation.

Fig. 1 depicts a sequence of identical oscillators with equal intervals d is crossing a single-span suspended beam at constant speed v. In this study, each of the oscillators is composed of a lumped mass supported by a spring–dashpot system, which is used to model either the front or rear half of a train car. Let the oscillator model has the following properties: m_w is the mass of wheel-set, m_v the lumped mass, c_v the damping coefficient, and k_v the stiffness coefficient. The loading function $p(x,t)$ is given as [7,13,14]:

$$p(x,t) = \sum_{k=1}^{N}(P - m_v\ddot{u}_{vk} - m_w\ddot{u})\delta(x - x_k)[H(t - t_g - t_k) - H(t - t_g - t_k - L/v)], \tag{9a}$$

$$m_v\ddot{u}_{vk} + c_v\dot{u}_{vk} + k_vu_{vk} = f_{vk}, \tag{9b}$$

$$f_{vk} = \begin{cases} k_v[u(x_k,t) + \gamma(x_k)] + c_v\dot{u}(x_k,t), & 0 \leqslant x_k (= v(t - t_g - t_k)) \leqslant L \\ k_v[u_{g,k}(t) + \gamma(x_k)] + c_v\dot{u}_{g,k}(t), & x_k < 0,\ x_k > L \end{cases} \tag{9c}$$

in which, $P = -(m_v+m_w)g$ is the lumped weight of a moving oscillator, g the gravity acceleration, δ the Dirac's delta function, $H(t)$ the unit step function, $k = 1,2,3,\ldots,N$th moving load on the beam, t_g the time lag for the first oscillator entering the suspension bridge from the left hand side, $t_k = (k-1)d/v$ the arrival time of the kth load into the beam, u_{vk} the vertical displacement of the kth lumped mass, f_{vk} the interaction force between the beam and the kth wheel mass, $u_{g,k}$ the vertical ground displacement under the kth load, $\gamma(x_k)$ the track irregularity (vertical profile), and x_k the position of the kth load along the rail line, as defined in Eq. (9c). Here, $x_k < 0$ represents the kth load is not yet entering the bridge, $0 \leqslant x_k (= v(t - t_g - t_k)) \leqslant L$ is running over the bridge deck, and $x_k > L$ has left the bridge.

2.2. Method of solution

As indicated in Eqs. (4), (7), and (9), they are a set of partial integro-differential equation associated with time-dependent boundary conditions and oscillator-related coupling terms. Let us focus on the time-dependent boundary problem, the total deflection $u(x,t)$ of the suspended beam can be divided into two parts: the *pseudo-static* displacement $U(x,t)$ and the *inertia-dynamic* deflection $u_d(x,t)$ [18], or

$$u(x,t) = U(x,t) + u_d(x,t). \tag{10}$$

Here, $U(x,t)$ represents the beam deformation caused by the *relative* support displacements applied statically [15], and $u_d(x,t)$ the *inertia-dynamic* deflection due to inertia effect of the beam structure [18]. By adopting this concept, substituting Eq. (10) into Eq. (7), and discarding all the dynamic terms and external loads, the pseudo-static equation of motion in terms of the pseudo-static displacement $U(x,t)$ can be written as follows:

$$EI\frac{\partial^4 U}{\partial x^4} - (T + \Delta T_s)\frac{\partial^2 U}{\partial x^2} + \alpha\int_0^L U\,\mathrm{d}x = \frac{\alpha L}{2}[u_0 + u_L] - \kappa(d_{xL} - d_{x0}). \tag{11}$$

And the pseudo-static response $U(x,t)$ in Eq. (11) has to satisfy the following *time-dependent* boundary conditions in Eqs. (4) [16–18]:

$$\begin{aligned} &U(0,t) = u_0, \quad U(L,t) = u_L, \\ &EIU''(0,t) = EIU''(L,t) = 0. \end{aligned} \tag{12}$$

Furthermore, introducing Eqs. (10) and (11) into Eq. (7) and removing the inertia force term of $(m\ddot{U} + c\dot{U})$ to the right hand side of Eq. (7), the equation of motion for a suspended beam is converted into

$$m\ddot{u}_d + c\dot{u}_d + EIu_d'''' - (T + \Delta T_s)u_d'' + \alpha\int_0^L u_d\,\mathrm{d}x = p(x,t) - (m\ddot{U} + c\dot{U}). \tag{13}$$

Since the pseudo-static displacement $U(x,t)$ has satisfied the *time-dependent* boundary conditions shown in Eqs. (12), introducing Eqs. (10) and (12) into Eqs. (4) yields the following *homogeneous* boundary conditions for the inertia-dynamic deflection $u_d(x,t)$:

$$\begin{aligned} &u_d(0,t) = u_d(L,t) = 0, \\ &EIu_d''(0,t) = EIu_d''(L,t) = 0. \end{aligned} \tag{14}$$

Obviously, once the pseudo-static displacement $U(x,t)$ is known, the response of *inertia-dynamic* deflection $u_d(x,t)$ in Eq. (13) associated with the homogeneous boundary conditions in Eqs. (14) can be solved by Galerkin's method and computed by the Newmark method in the time domain [13,21].

3. Solutions of pseudo-static and inertia-dynamic components

In this section, a closed form solution of pseudo-static deflection $U(x,t)$ for the suspended beam undergoing differential support movements will be first presented. Then, $-(m\ddot{U} + c\dot{U})$ in Eq. (13) can be regarded as equivalent dynamic forces acting on the suspended beam.

3.1. Solution of the pseudo-static displacement

To solve the integro-differential equation shown in Eq. (11), one can transform it into the following non-homogenous differential equation in terms of $U(x,t)$ as

$$\frac{\partial^4 U(x,t)}{\partial x^4} - \lambda^2\frac{\partial^2 U(x,t)}{\partial x^2} = \frac{\alpha L}{2EI}[u_0 + u_L] - \frac{\kappa}{EI}(d_{xL} - d_{x0}) - \frac{\alpha}{EI}\int_0^L U(x,t)\,\mathrm{d}x,$$

$$\lambda^2 = \frac{T + \Delta T_s}{EI}. \tag{15}$$

Then, the general solution for this fourth-order differential equation is expressed as

$$U(x,t) = d_0 \cosh \lambda x + d_1 \sinh \lambda x + c_0 + c_1 \frac{x}{L} + \frac{\alpha x^2}{2(T+\Delta T_s)} \left(\int_0^L U \, dx - \frac{L}{2}[u_0 + u_L] + \frac{\kappa}{\alpha}(d_{xL} - d_{x0}) \right). \tag{16}$$

And the exact solution can be solved as

$$U(x,t) = \left[u_0 + (u_L - u_0)\frac{x}{L} \right] + \left[\frac{L(d_{xL} - d_{x0})}{8y_0} \right] \frac{\beta(x,t)}{\chi}, \tag{17}$$

$$\beta(x,t) = \begin{cases} 1 + \dfrac{\lambda^2 x(x-L)}{2} - \dfrac{\cosh \lambda(x - L/2)}{\cosh(\lambda L/2)} & \text{for } T + \Delta T_s > 0 \\ 1 - \dfrac{|\lambda|^2 x(x-L)}{2} - \dfrac{\cos(|\lambda|(x - L/2))}{\cos(|\lambda| L/2)} & \text{for } T + \Delta T_s < 0, \end{cases} \tag{18a}$$

$$\chi(t) = \begin{cases} \dfrac{(T+\Delta T_s)(\lambda L)^2}{\alpha L^3} + \dfrac{(\lambda L)^2}{12} + \dfrac{\tanh(\lambda L/2)}{\lambda L/2} - 1 & \text{for } T + \Delta T_s > 0 \\ -\dfrac{(T+\Delta T_s)(|\lambda| L)^2}{\alpha L^3} - \dfrac{(|\lambda| L)^2}{12} + \dfrac{\tan(|\lambda| L/2)}{|\lambda| L/2} - 1 & \text{for } T + \Delta T_s < 0. \end{cases} \tag{18b}$$

The pseudo-static displacement shown in Eq. (17) reveals that the first term represents the *rigid body* displacement due to *vertical* support movements, and the second term means the *pseudo-static* natural deformation caused by the *relative horizontal* support movements. It is emphasized that the non-uniform nature of horizontal ground motion is of importance to earthquake-induced vibration of suspension bridges since it is usually assumed as *uniform* ground motion in seismic design.

3.2. Solution of inertia-dynamic deflection

Since the closed form solution of the *pseudo-static* deflection $U(x,t)$ has been presented in Eq. (17), the *inertia-dynamic* deflection $u_d(x,t)$ in Eq. (13) can be carried out by Galerkin's method. Thus the virtual work equation of Eq. (17) is expressed as [10]:

$$\int_0^L (m\ddot{u}_d + c\dot{u}_d + EIu_d'''' - (T+\Delta T_s)u_d'')\delta u_d \, dx + \left(\alpha \int_0^L u_d \, dx \right) \int_0^L \delta u_d \, dx = \int_0^L [p(x,t) - (m\ddot{U} + c\dot{U})]\delta u_d \, dx. \tag{19}$$

According to the homogeneous boundary conditions shown in Eqs. (14), the inertia-dynamic deflection (u_d) can be approximated by [7,10]

$$u_d(x,t) = \sum_{n=1} q_n(t) \sin \frac{n\pi x}{L}, \tag{20}$$

where $q_n(t)$ means the generalized coordinate associated with the nth assumed mode of the suspended beam. Substituting Eqs. (17) and (20) into Eq. (19) yields the following equation of motion for the nth generalized system:

$$m\ddot{q}_n + c\dot{q}_n + \left(\frac{n\pi}{L}\right)^2 \left[\left(\frac{n\pi}{L}\right)^2 EI + (T+\Delta T_s) \right] q_n + \Pi_n + \sum_{k=1}^{N} F_{vk}(\varpi_n, v, t) = \left[\sum_{k=1}^{N} F_k(\varpi_n, v, t) \right] - \frac{2}{n\pi}[m\ddot{\Upsilon}_n + c\dot{\Upsilon}_n], \tag{21}$$

$$\Pi_n = \frac{2\alpha L}{n\pi^2}(1 - \cos n\pi) \left[\sum_{k=1} \frac{1}{k}(1 - \cos k\pi) q_k \right], \tag{22a}$$

$$\Upsilon_n = \begin{cases} u_0 - u_L \cos n\pi + (\cos n\pi - 1)\dfrac{L(d_{xL} - d_{x0})}{8y_0\chi} \left(\dfrac{(\lambda L/n\pi)^4}{1 + (\lambda L/n\pi)^2} \right) & \text{for } T + \Delta T_s > 0 \\ u_0 - u_L \cos n\pi + (\cos n\pi - 1)\dfrac{L(d_{xL} - d_{x0})}{8y_0\chi} \left(\dfrac{(|\lambda| L/n\pi)^4}{1 - (|\lambda| L/n\pi)^2} \right) & \text{for } T + \Delta T_s < 0 \end{cases}, \tag{22b}$$

where the generalized forces of $F_k(\varpi_n, v, t)$ and $F_{vk}(\varpi_n, v, t)$ with respect to the kth sprung mass unit are

$$F_k(\varpi_n, v, t) = \frac{2P}{L}\psi_n(\varpi_n, t),$$

$$F_{vk}(\varpi_n, v, t) = \frac{2}{L}(m_v\ddot{u}_{v,k} + m_w\ddot{u}(x_k, t))\psi_n(\varpi_n, t),$$

$$\psi_n(\varpi_n, t) = \sin\varpi_n(t - t_g - t_k)[H(t - t_g - t_k) - H(t - t_g - t_k - L/v)], \tag{23a–c}$$

and $\varpi_n(= n\pi v/L)$. Let us consider a special case of uniform support motion, i.e., $u_0 = u_L$, $d_0 = d_L$, or $U(x, t) = u_0$, the generalized equation of motion in Eq. (21) is reduced to

(1) $n =$ odd,

$$m\ddot{q}_n + c\dot{q}_n + \left(\frac{n\pi}{L}\right)^2\left[\left(\frac{n\pi}{L}\right)^2 EI + (T + \Delta T_{s,\mathrm{syc}})\right]q_n + \frac{8\alpha L}{n\pi^2 m}\left[\sum_{k=1}\frac{q_k}{k}\right] + \sum_{k=1}^{N}(F_{vk}(\varpi_n, v, t) + F_{wk}(\varpi_n, v, t)) = \left[\sum_{k=1}^{N}F_k(\varpi_n, v, t)\right] - \frac{4}{n\pi}[m\ddot{u}_0 + c\dot{u}_0], \tag{24a}$$

(2) $n =$ even,

$$m\ddot{q}_n + c\dot{q}_n + \left(\frac{n\pi}{L}\right)^2\left[\left(\frac{n\pi}{L}\right)^2 EI + (T + \Delta T_{s,\mathrm{syc}})\right]q_n + \sum_{k=1}^{N}F_{vk}(\varpi_n, v, t) = \sum_{k=1}^{N}F_k(\varpi_n, v, t), \tag{24b}$$

$$\Delta T_{s,\mathrm{syc}} = -E_cA_c\frac{8y_0u_0}{L_cL}. \tag{24c}$$

Generally speaking, as a suspended beam is built far from the hypocenter of earthquakes, the additional cable force $\Delta T_{s,\mathrm{syc}}$ in Eq. (24c) induced by uniform vertical support motion is relatively small in comparison with the initial cable tension T due to dead loads, i.e., $T + \Delta T_{s,\mathrm{syc}} \simeq T$. It indicates that the symmetric modes of *inertia-dynamic* deflection in Eq. (24a) will be excited by uniform support motion.

4. Applications of incremental-iterative approach

As shown in Eqs. (21) and (22), the generalized equations for all the generalized coordinates are coupled due to the presence of the coupled terms, such as Π_n and $\sum_{k=1}^{N}F_{vk}(\varpi_n, v, t)$, in which the inertial forces of $F_{vk}(\varpi_n, v, t)$ are time-dependent on the location of the kth oscillator traveling over the suspended beam. Obviously, the computational efforts required for solving such a set of time-dependent coupled differential equations are tremendous in CPU time consuming for updating the structural matrices at each time step. This is especially true for the acceleration response, rather than the displacement response, is of concern in high speed rail bridges, for which the contribution of higher modes has to be included [24–27].

For the present purposes, let us treat the time-dependent terms of $(n\pi/L)^2\Delta T_s(t)$, $\sum_{k=1}^{N}F_{vk}(\varpi_n, v, t)$, and Π_n in Eq. (21) as pseudo forces, remove them to the right hand side of Eq. (21), and recast the differential equations of the suspended beam/oscillator coupling system as:

$$\begin{aligned} &m\ddot{q}_n + c\dot{q}_n + k_nq_n = p_n(t) - \Gamma_n(t),\\ &m_v\ddot{u}_{vk} + c_v\dot{u}_{vk} + k_vu_{vk} = f_{vk}, \end{aligned} \tag{25}$$

where

$$k_n = \left(\frac{n\pi}{L}\right)^2\left[\left(\frac{n\pi}{L}\right)^2 EI + T\right], \tag{26a}$$

$$p_n(t) = \left[\sum_{k=1}^{N}F_k(\varpi_n, v, t)\right] - \frac{2}{n\pi}[m\ddot{\Upsilon}_n + c\dot{\Upsilon}_n], \tag{26b}$$

$$\Gamma_n(t) = \left(\frac{n\pi}{L}\right)^2\Delta T_s + \Pi_n + \sum_{k=1}^{N}F_{vk}(\varpi_n, v, t), \tag{26c}$$

and k_n is the generalized stiffness associated with the nth generalized system, $p_n(t)$ the generalized force, and $-\Gamma_n(t)$ the *pseudo-forces* acting on the nth generalized system. Apparently, the original time-dependent coupled equations in Eq. (21) have been converted to an *uncoupled* equation associated with the nth generalized force $p_n(t)$ and *pseudo* force $-\Gamma_n$.

To perform nonlinear time-history procedure, the equations of motion in Eqs. (25) are first discretized by the Newmark method [21], and then the nth equivalent stiffness equation associated with the kth oscillator equation for the incremental step from time t to $t+\Delta t$ is expressed as

$$K_{n,eq} \times \Delta q_{n,t+\Delta t} = \Delta p_{n,t+\Delta t},$$
$$K_{v,eq} \times \Delta u_{vk,t+\Delta t} = \Delta f_{vk,t+\Delta t}, \tag{27}$$

where the equivalent stiffness of ($K_{n,\mathrm{eq}}$, $K_{v,\mathrm{eq}}$) and the *load increments* of ($\Delta p_{n,t+\Delta t}, \Delta f_{vk,t+\Delta t}$) are, respectively, given as follows:

$$K_{n,\mathrm{eq}} = a_0 m + a_1 c + k_n, \quad K_{v,\mathrm{eq}} = a_0 m_v + a_1 c_v + k_v, \tag{28a,b}$$

$$\Delta p_{n,t+\Delta t} = p_{n,t+\Delta t} - (\Gamma_{n,t+\Delta t} + R_{n,t}), \tag{28c}$$

$$R_{n,t} = k_n q_{n,t} - m(a_2 \dot{q}_{n,t} + a_3 \ddot{q}_{n,t}) - c(a_4 \dot{q}_{n,t} + a_5 \ddot{q}_{n,t}), \tag{28d}$$

$$\Delta f_{vk,t+\Delta t} = f_{vk,t+\Delta t} - r_{vk,t} \tag{28e}$$

$$r_{vk,t} = [k_v u_{vk,t} - m_v(a_2 \dot{u}_{vk,t} + a_3 \ddot{u}_{vk,t}) - c_v(a_4 \dot{u}_{vk,t} + a_5 \ddot{u}_{vk,t})]. \tag{28f}$$

and ($\Delta q_{n,t+\Delta t}, \Delta u_{vk,t+\Delta t}$) are the displacement increments generated at the incremental step, and ($R_{n,t}, r_{vk,t}$) the effective resistant forces. In respect to the total inertia-dynamic responses of ($q_{n,t+\Delta t}, \dot{q}_{n,t+\Delta t}, \ddot{q}_{n,t+\Delta t}$) for the nth generalized coordinate and ($u_{vk,t+\Delta t}, \dot{u}_{vk,t+\Delta t}, \ddot{u}_{vk,t+\Delta t}$) for the kth sprung mass at time $t+\Delta t$, they are, respectively, expressed as [10]

$$q_{n,t+\Delta t} = q_{n,t} + \Delta q_n, \quad u_{vk,t+\Delta t} = u_{vk,t} + \Delta u_{vk},$$

$$\dot{q}_{n,t+\Delta t} = \dot{q}_{n,t} + a_6 \ddot{q}_{n,t} + a_7 \ddot{q}_{n,t+\Delta t}, \quad \dot{u}_{vk,t+\Delta t} = \dot{u}_{vk,t} + a_6 \ddot{u}_{vk,t} + a_7 \ddot{u}_{vk,t+\Delta t},$$

$$\ddot{q}_{n,t+\Delta t} = a_0 \Delta q_n - a_2 \dot{q}_{n,t} - a_3 \ddot{q}_{n,t}, \quad \ddot{u}_{vk,t+\Delta t} = a_0 \Delta u_{vk} - a_2 \dot{u}_{vk,t} - a_3 \ddot{u}_{vk,t}, \tag{29}$$

with the following coefficients [21]:

$$a_0 = \frac{1}{\beta \cdot \Delta t^2}, \quad a_1 = \frac{\gamma}{\beta \cdot \Delta t}, \quad a_2 = \frac{1}{\beta \cdot \Delta t}, \quad a_3 = \frac{1}{2\beta} - 1, \quad a_4 = \frac{\gamma}{\beta} - 1,$$

$$a_5 = \frac{\Delta t}{2}\left(\frac{\gamma}{\beta} - 2\right), \quad a_6 = (1-\gamma)\Delta t, \quad a_7 = \gamma \cdot \Delta t \tag{30}$$

and $\beta = 0.25$ and $\gamma = 0.5$. The foregoing procedure can be modified to include the feature of *iteration* for removing the unbalanced forces as follows [10]:

$$K_{n,\mathrm{eq}} \times \Delta q^i_{n,t+\Delta t} = \Delta p^{i-1}_{n,t+\Delta t},$$

$$K_{v,\mathrm{eq}} \times \Delta u^i_{vk,t+\Delta t} = \Delta f^{i-1}_{vk,t+\Delta t}, \tag{31}$$

where ($\Delta q^i_{n,t+\Delta t}, \Delta u^i_{vk,t+\Delta t}$) represent the displacement increments of the nth generalized displacement ($q^i_{n,t+\Delta t}$) and the vertical displacement ($u^i_{vk,t+\Delta t}$) of the kth sprung mass at the ith iteration from time t to $t+\Delta t$, and ($\Delta p^{i-1}_{n,t+\Delta t}, \Delta f^{i-1}_{vk,t+\Delta t}$) are interpreted as the *unbalanced forces* during the following iterative steps. The unbalanced force $\Delta p^{i-1}_{n,t+\Delta t}$ is equal to the difference between the external force $p_{n,t+\Delta t}$ and the effective internal forces $f^{i-1}_{n,t+\Delta t}$ for the n-th generalized system of the suspended beam at time $t+\Delta t$, i.e.,

$$\Delta p^{i-1}_{n,t+\Delta t} = p_{n,t+\Delta t} - f^{i-1}_{n,t+\Delta t}, \quad f^{i-1}_{n,t+\Delta t} = \Gamma^{i-1}_{n,t+\Delta t} + R^{i-1}_{n,t+\Delta t}, \tag{32}$$

$$R^{i-1}_{n,t+\Delta t} = \begin{cases} k_n q^{i-1}_{n,t+\Delta t} - m(a_2 \dot{q}^{i-1}_{n,t+\Delta t} + a_3 \ddot{q}^{i-1}_{n,t+\Delta t}) - c(a_4 \dot{q}^{i-1}_{n,t+\Delta t} + a_5 \ddot{q}^{i-1}_{n,t+\Delta t}) & \text{for} \quad i = 1 \\ k_n q^{i-1}_{n,t+\Delta t} + m\ddot{q}^{i-1}_{n,t+\Delta t} + c\dot{q}^{i-1}_{n,t+\Delta t} & \text{for} \quad i > 1, \end{cases} \tag{33}$$

and the unbalanced force $\Delta f^{i-1}_{vk,t+\Delta t}$ for the kth sprung mass at time $t+\Delta t$ is equal to

$$\Delta f^{i-1}_{vk,t+\Delta t} = f^{i}_{vk,t+\Delta t} - r^{i-1}_{vk,t+\Delta t},$$

$$r^{i-1}_{\nu k,t+\Delta t}=\begin{cases} k_\nu u^{i-1}_{\nu k,t+\Delta t}-m_\nu(a_2\dot{u}^{i-1}_{\nu k,t+\Delta t}+a_3\ddot{u}^{i-1}_{\nu k,t+\Delta t})-c_\nu(a_4\dot{u}^{i-1}_{\nu k,t+\Delta t}+a_5\ddot{u}^{i-1}_{\nu k,t+\Delta t}) & \text{for } i=1\\ k_\nu u^{i-1}_{\nu k,t+\Delta t}+m_\nu\ddot{u}^{i-1}_{\nu k,t+\Delta t}+c_\nu\dot{u}^{i-1}_{\nu k,t+\Delta t} & \text{for } i>1 \end{cases}. \tag{34}$$

In this paper, an incremental-iterative procedure is used to solve the equivalent stiffness equations shown in Eqs. (31), which involves three major phases: *predictor*, *corrector* and *equilibrium-checking* [22,23]. The *predictor* is concerned with solution of the structural response increments of $(\Delta q^i_{n,t+\Delta t},\Delta u^i_{\nu k,t+\Delta t})$ for given loadings $(\Delta p^{i-1}_{n,t+\Delta t},\Delta f^{i-1}_{\nu k,t+\Delta t})$ from the equivalent structural stiffness equations. The *corrector* phase relates to recovery of the internal resistant forces $(f^{i-1}_{n,t+\Delta t},r^{i-1}_{\nu k,t+\Delta t})$ from the displacement increments of $(\Delta q^i_{n,t+\Delta t},\Delta u^i_{\nu k,t+\Delta t})$ and the total responses of $(q^i_{n,t+\Delta t},\dot{q}^i_{n,t+\Delta t},\ddot{q}^i_{n,t+\Delta t})$ and $(u^i_{\nu k,t+\Delta t},\dot{u}^i_{\nu k,t+\Delta t},\ddot{u}^i_{\nu k,t+\Delta t})$ made available in the predictor. In this phase, each of the pseudo force $\Gamma^{i-1}_{n,t+\Delta t}$, containing Π_n and $\sum_{k=1}^{N}F_{\nu k}(\varpi_n,\nu,t)$, is updated in an iterative way. In the *equilibrium-checking* phase, the effective internal forces of $(f^{i-1}_{n,t+\Delta t},r^{i-1}_{\nu k,t+\Delta t})$ computed from the *corrector* phase is compared with the external loads $(p_{n,t+\Delta t},f_{\nu k,t+\Delta t})$ in Eqs. (28), the difference being regarded as the unbalanced forces $(\Delta p^{i-1}_{n,t+\Delta t},\Delta f^{i-1}_{\nu k,t+\Delta t})$. Whenever the unbalanced forces are greater than preset tolerances, another iteration involving the three phases should be conducted.

5. Strategy for incremental-iterative dynamic analysis

In performing the dynamic response analysis of structures containing seismic ground motions, two sets of structure responses have to be computed each for the pseudo-static response and for the inertia-dynamic response. The incremental-iterative procedure of nonlinear dynamic analysis for vehicle–bridge system shaken by earthquakes is summarized as follows:

(1) Treat the *pseudo-static* displacement $U(x,t)$ derived in Section 3.1 as an exciting source to the equivalent dynamic force $(-m\ddot{U}-c\dot{U})$ to act on the beam–oscillator coupling system (see Section 3.2).
(2) Transform the governing differential equation in Eq. (13) into a set of coupled equations of generalized system as Eq. (21) and then remove the coupled terms to the right hand side of Eq. (21) to form a set of uncoupled equations of motion (see Eq. (25)).
(3) Discretize each of the uncoupled equations into an equivalent stiffness equations using Newmark's method (see Eq. (27)).
(4) Perform the iterative procedure proposed in Section 4 to compute the *inertia-dynamic* response of the suspended beam.
(5) Update the total responses of the suspended beam by combining the pseudo-static and inertia-dynamic components of the beam response by using Eq. (10).
(6) Compute the dynamic response of moving oscillators at each iteration.
(7) Check the unbalanced forces to reach preset tolerances. As the root mean square of the sum of the generalized unbalanced forces is larger than the preset tolerances, go to step (4) for preceding the next iteration to remove the unbalanced forces.
(8) Repeat the steps (4)–(7) for other time instants.

6. Numerical investigations

Fig. 1 shows a series of moving oscillators with equal intervals d are crossing a single-span suspended beam at constant speed v. The properties of the suspended beam and sprung mass unit are listed in Tables 1 and 2, respectively. As shown in Table 1, the first natural frequency (Ω_1) of anti-symmetric mode of the suspended beam is lower than the second one (Ω_2) of symmetric bending mode. It means the cable tension has developed a strengthening effect on the first symmetric bending mode of the suspended beam.

To take into account the random nature and characteristics of track irregularity that can amplify the vibration response of a moving train, the following *power spectrum density* (PSD) function for track class 6 designed by *Federal Railroad Administration* (USA) [13] is given to simulate the vertical profile of track geometry variations

$$S(\Omega)=\frac{A_v\Omega_c^2}{(\Omega^2+\Omega_r^2)(\Omega^2+\Omega_c^2)},$$

Table 1
Properties and natural frequencies of the suspended beam.

L (m)	EI (kN m^2)	E_cA_c (kN)	m (t/m)	c (kN s/m/m)	y_0 (m) [y_0/L]	E_cA_c/L_e (kN/m)	Ω_1 (Hz)	Ω_2 (Hz)
125	2.3×10^8	6.0×10^7	16	4.61	12.5 [0.10]	4.437×10^5	1.55	1.73

Table 2
Properties of moving oscillator and resonant speeds.

N	d (m)	P (kN)	m_w (t)	m_v (t)	c_v (kN s/m)	k_v (kN/m)	$v_{res,1}$ (km/h)	$v_{res,2}$ (km/h)
16	27	340	4.7	30.0	5.2	157	152	168

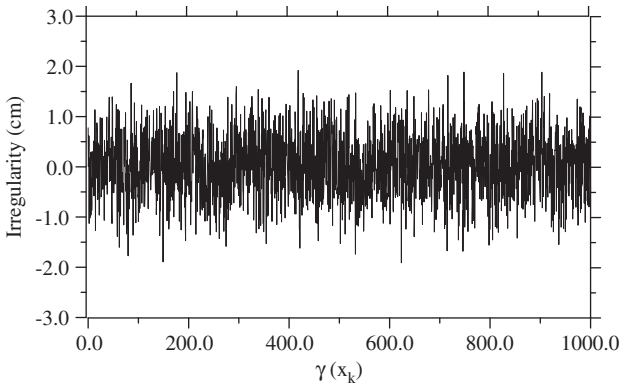

Fig. 2. Track irregularity (vertical profile).

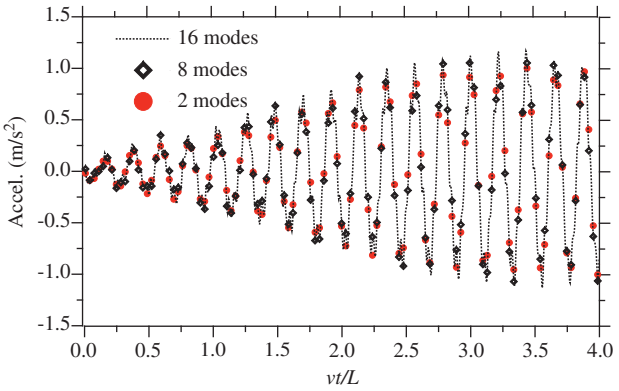

Fig. 3. Test of convergence.

where $\Omega =$ spatial frequency, and A_v ($= 1.5 \times 10^{-6}$ m), Ω_r ($= 2.06 \times 10^{-6}$ rad/m), and Ω_c ($= 0.825$ rad/m) are relevant parameters. Fig. 2 shows the vertical profile of track irregularity for the simulation of track geometry variations in this study.

6.1. Resonance of acceleration response

As the *passage frequency* ($= v/d$) of train loadings matches any of natural frequencies (Ω_i) of a bridge, the resonant response of the bridge will be developed [24–26], and the resonant speed of the train is denoted as $v_{res,i} = \Omega_i d$ [25,26]. This is so called *resonance phenomenon* for train-induced response of railway bridges [13,14]. To demonstrate the resonance phenomenon of a suspended beam induced by moving loads with identical intervals, let the moving oscillators pass through the suspended beam with the first two resonant speeds, i.e., $v_{res,1} = \Omega_1 d = 41.9$ m/s ($= 152$ km/h) and $v_{res,2} = \Omega_2 d = 46.6$ m/s ($= 168$ km/h), respectively. Generally speaking, the acceleration response of vehicle–bridge system is usually used to evaluate the running safety of high speed trains over railway bridges [24–26]. In order to verify that a sufficient number of modes of vibration in Eq. (20) has been used in the analysis, we first compute the acceleration response at the first quarter-point of the main beam under a series of moving oscillators with the first resonant speed using either 2, 8, or 16 modes. As can be seen from Fig. 3, the use of 16 modes is considered sufficient. For this reason, the same number of modes will be used in all the examples to follow.

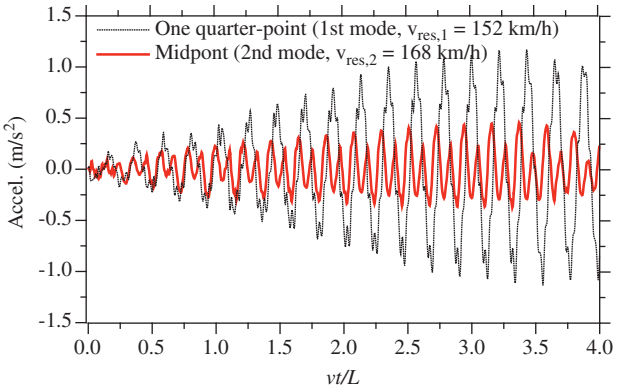

Fig. 4. Time history responses of beam acceleration.

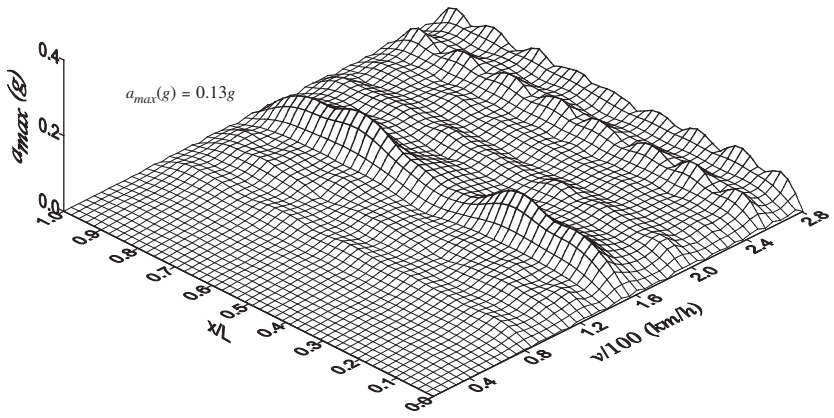

Fig. 5. $a_{\max}$–v–x/L plot of the suspended beam due to multiple moving oscillators.

In addition, the time history responses of acceleration at the positions of mid-span and one quarter of the suspended beam have been depicted in Fig. 4 as well. As was mentioned earlier, both the acceleration responses are built up as there are more moving oscillators passing through the beam. But the resonant response at the mid-span is significantly smaller than that at one-quarter point. One reason for this is that as a series of moving loads, with an equal interval ($d = 27$ m) far smaller than the bridge span length ($L = 125$ m), pass through the suspension bridge, the simultaneous presence of multiple loads moving over the bridge deck may exert a *suppression action* on the first symmetric mode (i.e., the second bending mode), which may cause the mid-span acceleration of the bridge deck to be less severe compared with the other resonant case involving the anti-symmetric mode.

For the purpose of illustration, a three-dimensional (3D) plot for the maximum acceleration response ($a_{\max}$) along the beam span (x/L) against moving speed (v) for the vibrating beam has been drawn in Fig. 5. Such a 3D plot will be called $a_{\max}$–v–x/L plot in the following examples. As can be seen from the two resonant peaks, the maximum acceleration response of the suspended beam at the speed of 152 km/h is governed by the anti-symmetrical modes that have been excited. Moreover, the maximum vertical accelerations of sprung mass units traveling over the suspended beam with various speeds have been plotted in Fig. 6. Such a plot is called $a_{v,\max}$–v plot. The maximum acceleration response of the moving oscillators slightly reaches its maximum value in the vicinity of 152 km/h due to the resonant response of the suspended beam.

6.2. Effect of uniform support motion

To investigate the influence of seismic ground motion on train-induced vibration of suspension bridges, the far-field ground motions of TAP003 station recorded at Taipei during the 1999 Chi–Chi Earthquake in Taiwan [13] are used to simulate the seismic support inputs. The histograms of ground acceleration, containing both the NS horizontal and vertical components, have been plotted in Figs. 7(a) and (b), respectively. As can be seen from the ground acceleration records depicted in Fig. 7(a), the intensive zone of vertical ground acceleration occurs early compared to that of horizontal

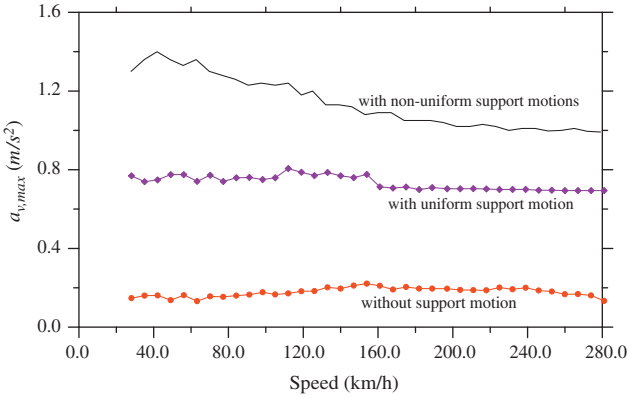

Fig. 6. Maximum acceleration of moving sprung masses.

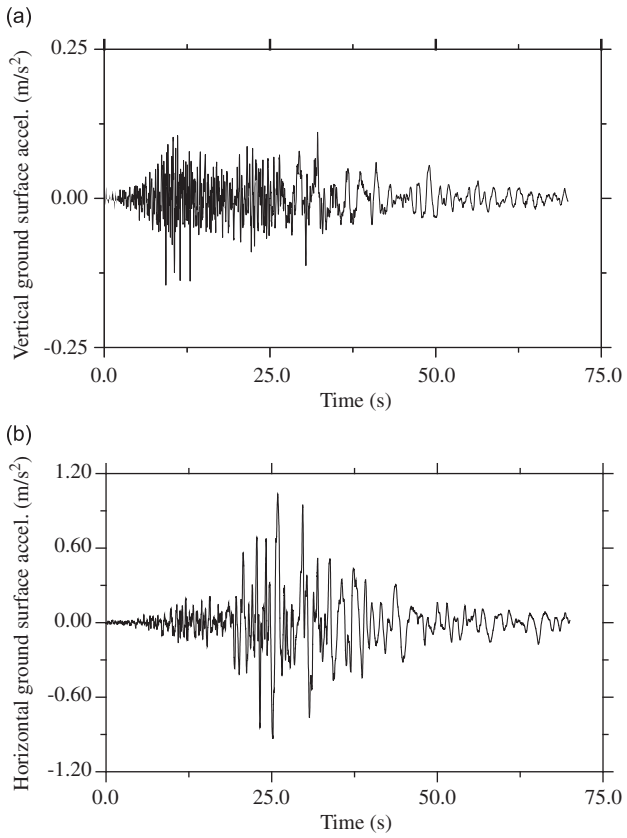

Fig. 7. Histograms of ground acceleration of TAP003 station: (a) vertical and (b) NS horizontal.

component in Fig. 7(b) due to the fact that the primarily wave (*P*-wave) produced by earthquakes travels faster than the shear one (*S*-wave).

Let us consider the special case of *uniform* support motion, i.e., $u_0 = u_L$, $d_0 = d_L$, with various time lags of t_g for the sprung mass units entering the suspended beam at the first resonant speed of $v_{\text{res},1}$ (= 152 km/h), Fig. 8 shows the maximum acceleration amplitude in $a_{\max}$–x/L plot of the beam will occur at the critical time lag of 12 s, which is just inside the intensive zone of vertical ground motions depicted in Fig. 7(a). This critical time of 12 s, therefore, will be used as the time lag for the moving oscillators to start entering the suspended beam in this example. As shown in the $a_{\max}$–v–x/L plot of Fig. 9 and the corresponding $a_{v,\max}$–v plot in Fig. 6, the inclusion of uniform ground motions can totally amplify both the acceleration amplitudes of the suspended beam and sprung masses. Moreover, from the acceleration amplitudes plotted in Fig. 9, most of the symmetric modes are excited by the uniform ground support motion, as was concluded in Section 3.2.

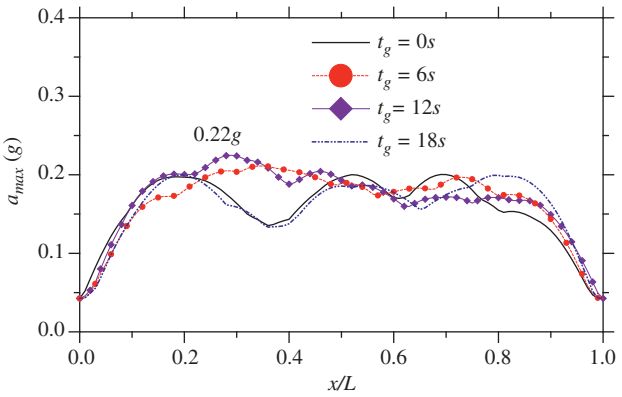

Fig. 8. Effect of time lags due to moving oscillators.

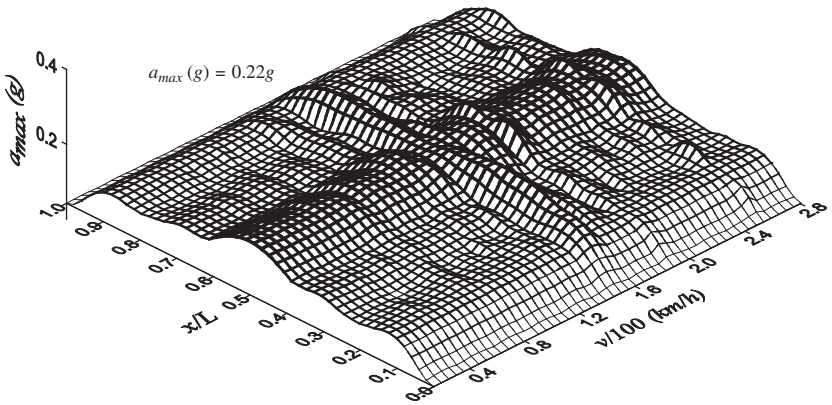

Fig. 9. Effect of vertical uniform support motion on $a_{\max}$–v–x/L plot.

6.3. *Effect of multiple support motions*

Due to soil conditions at local construction site of bridge foundations depicted in Fig. 1, let us assume that the intensities of seismic ground inputs transmitting into the right bridge support have comparative attenuation, say, $u_L = 0.8u_0$, $d_L = 0.7d_0$, compared to the left one. Thus, the suspended beam will undergo the action of multiple support movements during this earthquake excitation. As can be seen, the intensive zone of horizontal ground movements appears nearby 25 s. For this reason, this critical time lag is adopted for the moving oscillators to start entering the suspended beam in the following examples. Considering the moving effect of the multiple oscillators, Fig. 10 shows the $a_{\max}$–v–x/L plot for the suspended beam shaken by the present seismic excitations. By comparing the maximum acceleration amplitudes in Fig. 9 with those in Fig. 10, the amplification effect of multiple support excitations involving horizontal and vertical components is rather significant on the response of the suspended beam. Especially in the vicinity of three-quarters span of the suspended beam at the first resonant speed $v_{\text{res},1}$, there exists a noticeable peak acceleration amplitude ($=0.34g$). Moreover, the corresponding $a_{v,\max}$–v plot has been plotted in Fig. 6 as well, from which the maximum acceleration responses of sprung masses are totally amplified, especially at the lower speeds (<50 km/h). It means that as a series of sprung masses pass through a suspended beam with lower speeds, they will require more time to cross the long-span beam so that they have more chance to experience the excessive vibration induced by the intensively horizontal support excitations.

6.4. *Response reduction of suspended beams by adjusting cable sags*

As was expressed in Eq. (21), the generalized stiffness containing $(T+\Delta T_s)(n\pi/L)^2$ and Π_n strongly depends on both the cable sag ratio (y_0/L) and the cable stiffness parameter (E_cA_c/L_c). Besides, an important conclusion from Eqs. (7) and (8) indicates that reducing the cable stiffness parameter may relieve the horizontal component $(T+\Delta T_s)$ of cable tension due to differential support movements, and that increasing the cable sag ratio (y_0/L) can strengthen the bending stiffness of the suspended beam. This finding gives us a hint that we can appropriately adjust both the sag ratio (y_0/L) and cable stiffness (E_cA_c/L_c) to diminish the seismic ground excitation into the suspended beam. For this reason, let us consider the following

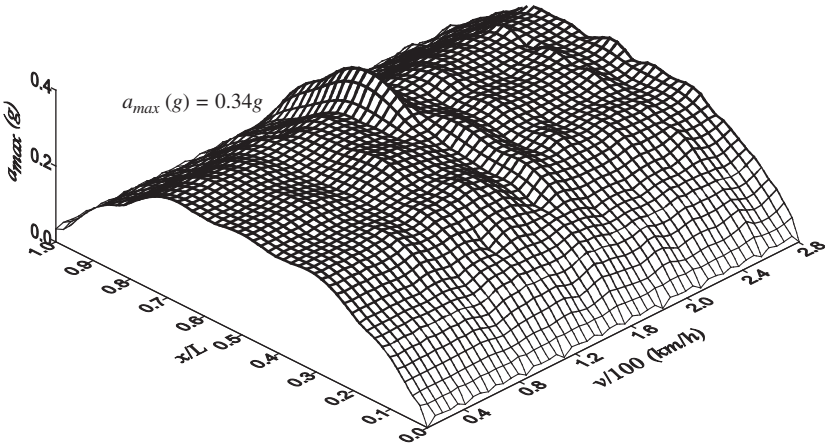

Fig. 10. Effect of multiple support motions on a_{max}–v–x/L plot.

Table 3
Properties and natural frequencies of new suspended beams.

L (m)	EI (kN m^2)	E_cA_c (kN)	m (t/m)	c (kN s/m/m)	y_0 (m) [y_0/L]	E_cA_c/L_e (kN/m)	Ω_1 (Hz)	Ω_2 (Hz)
125	2.3×10^8	2.95×10^7	16	4.61	18.75 [0.15]	1.981×10^5	1.55	1.73
125	2.3×10^8	1.88×10^7	16	4.61	25 [0.20]	1.115×10^5	1.55	1.73
125	2.3×10^8	1.4×10^7	16	4.61	31.25 [0.25]	7.143×10^4	1.55	1.73

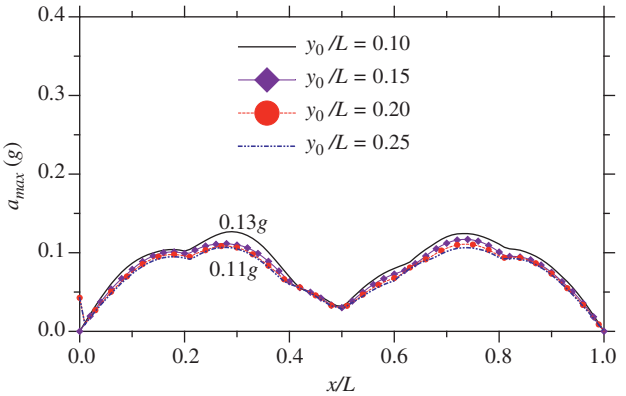

Fig. 11. Effect of cable sag ratios on a_{max}–x/L plot (without earthquake).

condition for a new suspended beam with adjustable cable sag that its first two frequencies have to remain identical with those of the initial one. By this requirement, Table 3 lists the sectional properties of suspension cables for the new suspended beam with three types of cable sags. Let the moving oscillators transverse each of the new suspended beams given in Table 3 with the first resonant speed of $v_{res,1}$ (= 152 km/h), respectively. The corresponding a_{max}–x/L plots of these suspended beams have been drawn in Fig. 11. The results show that the variations of acceleration amplitude are limited in a quite small range even though the cable sag ratio (y_0/L) reaches a maximum value of 0.25.

Next, let the multiple seismic support inputs used in Section 6.3 shake the new suspended beams. Consider the first resonant speed of $v_{res,1}$ (= 152 km/h), the corresponding a_{max}–x/L plots and $a_{v,max}$–v plots have been depicted in Figs. 12 and 13, respectively. Obviously, under the condition of identical frequencies for the suspended beams, the increase of cable sag ratios (y_0/L) is beneficial to suppressing both the maximum acceleration of the beam/oscillator system.

6.5. *Effects of seismic wave propagation*

Let us assume that the *P*-wave velocity for vertical support excitation is 500 m/s, and the *S*-wave velocity 100 m/s for horizontal seismic support input. Consider the case that the arrival of seismic wave at the right bridge support is always

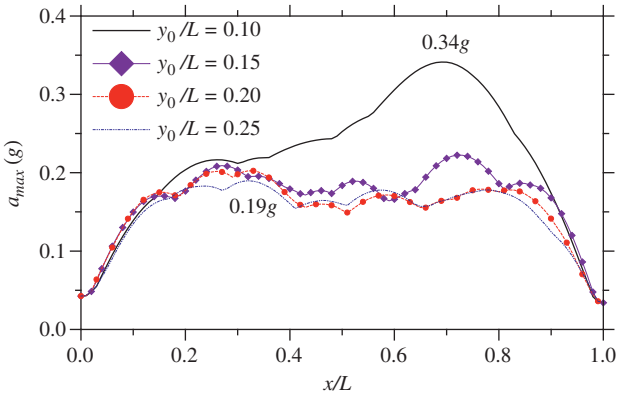

Fig. 12. Effect of cable sag ratios on a_{max}–x/L plot (with earthquake).

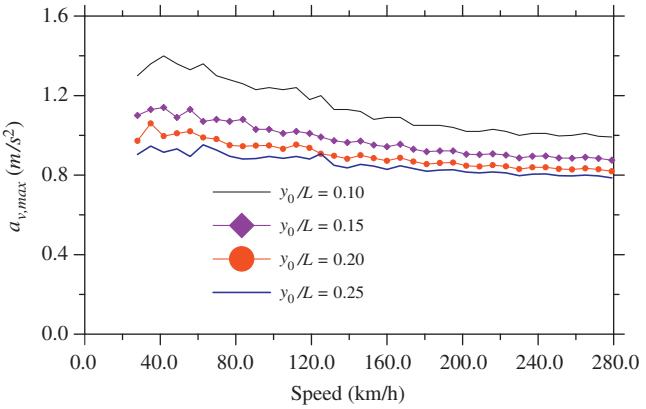

Fig. 13. Effect of cable sags on maximum acceleration of sprung masses.

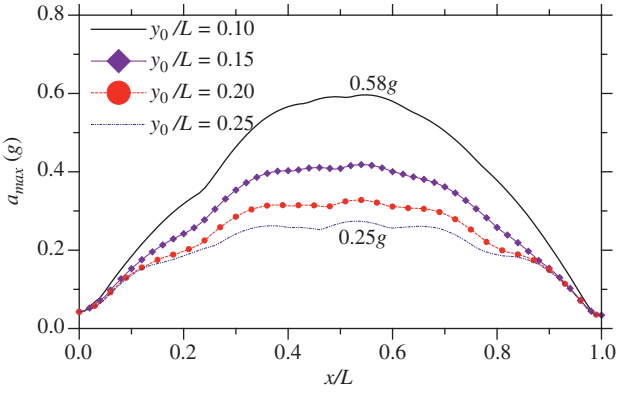

Fig. 14. Effect of seismic wave propagation on a_{max}–x/L plot.

behind the left one with a time delay of L/s_w (s_w = seismic wave speed). Fig. 14 shows the a_{max}–x/L plots for the new suspended beams (described in Table 3) subject to the simultaneous action of the train loadings moving at $v_{res,1}$ (= 152 km/h) and the present seismic ground motions. Besides, the corresponding $a_{v,max}$–v plots for the moving oscillators over the new suspended beams described in Section 6.4 have been plotted in Fig. 15. Although the acceleration amplitudes of these suspended beams are amplified significantly due to seismic wave passage effect, under the condition of identical bridge frequencies, the increase of cable sags is available to reduce both the acceleration responses of the suspended beam/oscillator system. From the trend of $a_{v,max}$–v plot shown in Fig. 15, as a train crosses a suspension bridge during earthquakes, raising the moving speed can help the vehicles experience less vertical excitations induced by the vibrating beam.

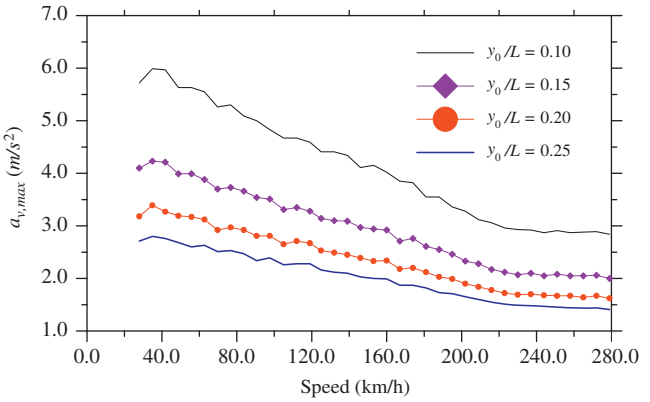

Fig. 15. Effect of seismic wave propagation on maximum acceleration of sprung masses.

7. Concluding remarks

Considering non-uniform characteristics of multiple support excitations, the interaction responses of a single-span suspended beam subject to multiple moving oscillators have been carried out using a *pseudo-decomposition* concept. By treating the nonlinear coupled terms as the pseudo forces, the coupled differential equations for all of the generalized systems are first converted by Newmark's β method to a set of equivalent stiffness equations of motion with the generalized forces and pseudo forces. Finally, these equivalent equations are solved by the proposed incremental-iterative procedure involving the three phases of predictor, corrector, and equilibrium-checking. From this study, the following conclusions are reached:

1. As the *passage frequency* (v/d) caused by a train traveling over a bridge coincides with any of bridge frequencies, resonance will be developed on the bridge.
2. As successive moving oscillators pass through a suspended beam at the resonant speed of the first symmetric mode, the simultaneous presence of multiple loads over the beam may exert a *suppression action* on the symmetric bending mode, which may cause the mid-span acceleration of the beam to be less severe compared with the other resonant case involving the anti-symmetric mode.
3. From the derived *pseudo-static* response, non-uniform horizontal ground motions may affect the response of a suspended beam. Such a fact is often neglected by the assumption of uniform seismic ground motion in conventional bridge design.
4. Under the condition of identical frequencies for new suspended beams, the increase of cable sags will not produce significant difference on the beam responses due to train loadings.
5. Although the seismic wave passage effect may totally amplify the interaction responses of the suspended beam/oscillator coupling system, under the condition of identical bridge frequencies, appropriate adjustments by increasing cable sags but reducing cable stiffness can help mitigate the earthquake-induced response of the train/bridge system.

Acknowledgment

This research was partly sponsored by a grant (NSC 97-2221-E-032-022-MY2) from the *National Science Council*, *Taiwan*, ROC.

References

[1] A.M. Abdel-Ghaffar, Vertical vibration analysis of suspension bridges, *ASCE Journal of Structural Division* 106 (1980) 2053–2075.
[2] A.M. Abdel-Ghaffar, L.I. Rubin, Suspension bridge response to multiple-support excitations, *ASCE Journal of Engineering Mechanic Division* 108 (1982) 419–435.
[3] A.M. Abdel-Ghaffar, L.I. Rubin, Vertical seismic behaviour of suspension bridges, *Earthquake Engineering and Structural Dynamics* 11 (1983) 1–19.
[4] M. Shrikhande, V.K. Gupta, Dynamic soil-structure interaction effects on the seismic response of suspension bridges, *Earthquake Engineering and Structural Dynamics* 28 (1999) 1383–1403.
[5] S.M. Allam, T.K. Datta, Response spectrum analysis of suspension bridges for random ground motion, *ASCE Journal of Bridge Engineering* 7 (2000) 325–337.
[6] A. Pugsley, *The Theory of Suspension Bridges*, second ed., Edward Arnold Ltd., London, 1957.
[7] L. Frýba, *Vibration of Solids and Structures under Moving Loads*, third ed., Thomas Telford, London, 1999.
[8] J. Vellozzi, Vibration of suspension bridges under moving loads, *ASCE Journal of Structural Division* 93 (1967) 123–138.
[9] T. Hayashikawa, N. Watanabe, Suspension bridge response to moving loads, *ASCE Journal of Engineering Mechanics* 108 (1982) 1051–1066.
[10] J.D. Yau, Y.B. Yang, Vibration of a suspension bridge installed with a water pipeline and subjected to moving trains, *Engineering Structures* 30 (2008) 632–642.

[11] D. Bryja, P. Sniady, Spatially coupled vibrations of a suspension bridge under random highway traffic, *Earthquake Engineering and Structural Dynamics* 20 (1991) 999–1010.
[12] P.K. Chatterjee, T.K. Datta, C.S. Surana, Vibration of suspension bridges under vehicular movements, *ASCE Journal of Structural Division* 120 (1993) 681–703.
[13] Y.B. Yang, J.D. Yau, Y.S. Wu, *Vehicle–bridge Interaction Dynamics*, World Scientific, Singapore, 2004.
[14] Y.B. Yang, J.D. Yau, L.C. Hsu, Vibration of simple beams due to trains moving at high speeds, *Engineering Structures* 19 (1997) 936–944.
[15] H. Xia, Y. Han, N. Zhang, W. Guo, Dynamic analysis of train-bridge system subjected to non-uniform seismic excitations, *Earthquake Engineering and Structural Dynamics* 35 (2006) 1563–1579.
[16] R.W. Clough, J. Penzien, *Dynamics of Structures*, McGraw-Hill, New York, 1975.
[17] R.D. Mindlin, J.E. Goodman, Beam vibrations with time dependent boundary conditions, *ASME Journal of Applied Mechanics* 17 (1950) 377–380.
[18] J.T. Chen, S.W. Chyuan, D.W. You, F.C. Wong, Normalized quasi-static mass—a new definition for multi-support motion problems, *Finite Elements in Analysis and Design* 26 (1997) 129–142.
[19] S.G. Buonopane, D.P. Billington, Theory and history of suspension bridge design from 1823 to 1940, *ASCE Journal of Structural Engineering* 119 (1993) 954–977.
[20] H.M. Irvine, *Cable Structures*, MIT Press, Cambridge, 1981.
[21] N.M. Newmark, A method of computation for structural dynamics, *ASCE Journal of Engineering Mechanical Division* 85 (1959) 67–94.
[22] Y.B. Yang, S.R. Kuo, *Theory and Analysis of Nonlinear Framed Structures*, Prentice-Hall, Singapore, 1994.
[23] Y.B. Yang, T.Y. Lee, I.C. Tsai, Response of multi degree of freedom structures with sliding supports, *Earthquake Engineering and Structural Dynamics* 19 (1990) 739–752.
[24] J.D. Yau, Y.B. Yang, Vertical accelerations of simple beams due to successive loads traveling at resonant speeds, *Journal of Sound and Vibration* 289 (2006) 210–228.
[25] J.D. Yau, Vibration of parabolic tied-arch beams due to moving loads, *International Journal of Structural Stability and Dynamics* 6 (2006) 193–214.
[26] J.D. Yau, Vibration of arch bridges due to moving loads and vertical ground motions, *Journal of Chinese Institute of Engineers* 29 (2006) 1017–1027.
[27] J.D. Yau, Train-induced vibration control of simple beams using string-type tuned mass dampers, *Journal of Mechanics* 23 (2007) 329–340.